# Nondipole asymmetries of K-shell photoelectrons of Kr, $Br_2$, and $BrCF_3$

S. H. Southworth, R. W. Dunford, E. P. Kanter, B. Krässig, L. Young
*Argonne National Laboratory, Argonne, IL 60439, USA*

L. A. LaJohn, R. H. Pratt
*Department of Physics and Astronomy, University of Pittsburgh, Pittsburgh, PA 15260, USA*

**Abstract**

The nondipole asymmetries of Kr 1s and Br K-shell photoelectrons of $Br_2$ and $BrCF_3$ were measured and compared with first-order retardation calculations within the independent-particle approximation. The measured asymmetries agree well with calculations and demonstrate the importance of screening on the normalizations and phase shifts of the continuum functions. Only small deviations are observed between the molecular Br K-shell measurements and calculations for atomic Br 1s.

*Key words:* X ray, K shell, photoelectron angular distribution, nondipole
*PACS:* 32.80.Fb, 33.60.Fy, 33.80.Eh

Photoionization dynamics of atoms and small molecules has been extensively studied using tunable synchrotron radiation to measure angle-integrated cross sections and dipole anisotropies of photoelectron angular distributions [1,2]. Cross sections and dipole anisotropies can be calculated using the dipole approximation to the photon-electron interaction in which the amplitude of the radiation field is assumed to be constant over the spatial dimensions of the absorbing charge distribution [3,4]. As a consequence of retardation, the amplitude of the radiation field varies over the charge distribution and induces higher-multipole interactions. First-order corrections to the dipole approximation include interference of electric-dipole (E1) amplitudes with electric-quadrupole (E2) and magnetic-dipole (M1) amplitudes. For a linearly-polarized photon beam, the differential cross section can be expressed as [5]

$$\frac{d\sigma}{d\Omega}(\theta,\phi) = \frac{\sigma}{4\pi}[1+\beta(3\cos^2\theta-1)/2 + (\delta+\gamma\cos^2\theta)\sin\theta\cos\phi], \quad (1)$$

where $\sigma$ is the angle-integrated cross section, $\beta$ is the dipole anisotropy parameter, and $\delta$ and $\gamma$ characterize the asymmetries resulting from E1-E2 and E1-M1 cross terms. $\theta$ and $\phi$ are the polar and azimuthal angles of the photoelectron momentum vector in a coordinate system with the positive x axis along the photon propagation vector $\mathbf{k}$ and the z axis along the linear polarization vector $\boldsymbol{\epsilon}$. The $\delta$ and $\gamma$ parameters characterize asym-

metries with respect to reversal of the direction of $\mathbf{k}$. Nondipole asymmetries are sensitive to variations in the magnitudes and phases of E1, E2, and M1 photoionization amplitudes and provide information on photoionization dynamics that complements or extends information from cross sections and dipole anisotropies [6,7].

We have developed a photoelectron spectrometer system with four parallel-plate electron analyzers positioned on a rotation platform at the magic angle with respect to the rotation axis and with the rotation axis perpendicular to $\mathbf{k}$ and $\boldsymbol{\epsilon}$. The $\beta$, $\delta$, and $\gamma$ parameters can be determined from photoelectron intensities measured at selected angles of the rotation axis. The spectrometer and experimental methods are described in Ref. [8] along with measured and calculated nondipole asymmetries of Kr 1s photoelectrons. Here we compare the Kr 1s asymmetries with those of Br K-shell photoelectrons of molecular $Br_2$ and $BrCF_3$. The molecular Br studies were motivated by the measurements and theoretical calculation of nondipole asymmetries of $N_2$ K-shell photoelectrons that greatly exceed the calculated asymmetries of atomic N 1s [9]. A similar "extra-atomic" effect was measured for C K-shell photoelectrons of CO [10].

The nondipole asymmetries of Kr 1s photoelectrons were measured over the 11–8000 eV kinetic energy range using 14.3–22.3 keV X rays and compared with theoretical calculations [8]. The measured asymmetries agree well with both full multipole relativistic and nonrelativistic first-order retardation calculations within the independent-particle approximation (IPA). In the kinetic energy region from threshold to 2000 eV, the essential physics appears to be well described by the first-order retardation nonrelativistic IPA model [11]. Two continuum waves are treated, $1s \rightarrow \epsilon p$ by E1 interaction and $1s \rightarrow \epsilon d$ by E2 interaction. The angular distribution is simplified to the form with $\beta = 2$, $\delta = 0$, and $\gamma$ can be expressed in atomic units as [5]

$$\gamma = 3\alpha\omega\frac{Q}{D}\cos(\delta_2 - \delta_1), \qquad (2)$$

where $\alpha$ is the fine-structure constant, $\omega$ is the photon energy, $D, Q$ are the radial dipole and quadrupole matrix elements, and $\delta_{1,2}$ are the

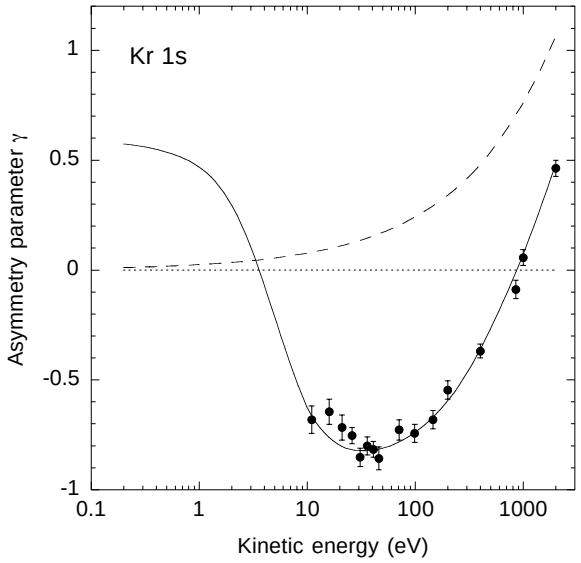


Fig. 1. Measurements and calculations [11] of the Kr 1s nondipole asymmetry parameter $\gamma$. The dashed curve is the $12(v/c)$ prediction of the point-Coulomb model. The solid curve includes screening within the nonrelativistic first-order retardation independent-particle approximation.

asymptotic phase shifts. The measured and calculated $\gamma$ parameters agree well and are plotted in Fig. 1 along with the point-Coulomb model that predicts $\gamma = 12(v/c)$, where $v$ is the photoelectron velocity. The point-Coulomb model is inaccurate at low kinetic energies where screening affects the normalizations and asymptotic phase shifts of the continuum functions. The $\gamma$ parameter is negative over ≈5–800 eV, i.e., the angular distribution is tilted backwards with respect to $\mathbf{k}$, contrary to the intuitive idea of the photoelectron being pushed forward by the photon momentum. Inspection of the normalizations and phase shifts of the continuum functions indicates the presence of an IPA shape resonance in the $\epsilon d$ channel that produces rapid variation of the calculated $\gamma$ parameter over the 1–10 eV region.

The nondipole asymmetries of Br K-shell photoelectrons of $Br_2$ and $BrCF_3$ were measured over the 20–950 eV kinetic energy range using 13.5–14.5 keV X rays. $BrCF_3$ was obtained from a compressed gas cylinder and $Br_2$ vapor was obtained from a vacuum-distilled liquid sample. A photoelectron and Auger electron spectrum of $Br_2$ is

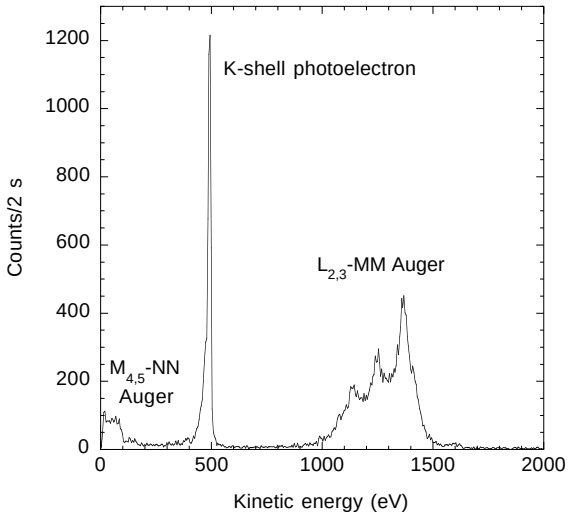


Fig. 2. K-shell photoelectron and Auger electron spectra of $Br_2$ recorded using 13.974 keV X rays. The spectrum is summed over the four electron analyzers and is uncorrected for their collection efficiencies, which are proportional to kinetic energy.

plotted in Fig. 2. The Auger-electron intensities varied 1–3% with angle and were used to make small corrections to the photoelectron intensities as explained in Ref. [8]. The measured values of $\gamma + 3\delta$ are plotted in Fig. 3 along with theoretical calculations for atomic Br 1s. Full multipole relativisitic IPA calculations produced values for the asymmetry parameters $B_n$ defined in the theoretical formulation of Ref. [12]. Referring to the first-order retardation expression in Eq. 1, the equivalent combination of asymmetry parameters is $\gamma + 3\delta = 3B_1 - 2B_3$. The second-order retardation calculation, in which the $B_4$ asymmetry parameter also contributes, was negligibly different than the first-order results for kinetic energies up to 1000 eV.

Overall, the measured nondipole asymmetries for $Br_2$ and $BrCF_3$ agree with each other and with the calculation for atomic Br 1s. The measurements tend to be slightly higher than the atomic calculation for kinetic energies below 100 eV but do not show a dramatic departure from the atomic model as observed for $N_2$ and CO K-shells using soft X rays [9,10]. The measurements and calculations for Br K-shell are similar to those of Kr in Fig. 1. The rapid drop in the calculated asym-

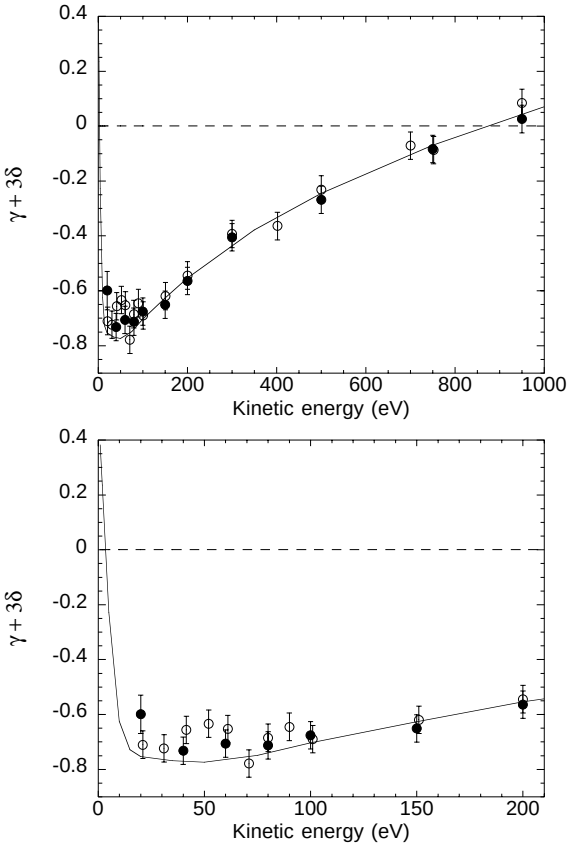


Fig. 3. Nondipole asymmetry parameters measured for Br K-shell photoelectrons of $Br_2$ (solid circles) and $BrCF_3$ (open circles) compared with first-order retardation calculations for atomic Br 1s (solid line). The top figure shows the full energy range and the bottom figure shows the results below 210 eV.

metry from positive to negative values over the 1–10 eV kinetic energy region is associated with an IPA shape resonance in the $\epsilon d$ channel for both Kr and Br. Due to its proximity to the nucleus and lack of penetration by orbitals on neighboring atoms, the Br 1s atomic orbital remains highly localized within the molecules. The observation that the molecular nondipole asymmetries are similar to that calculated for Br 1s suggests that the $\epsilon p$ and $\epsilon d$ continuum waves of the atomic model are not significantly modified by rescattering in the molecular field produced by neighboring atoms ("electron optical" effects [13]).

The $N_2$ and CO experiments [9,10] used 300–700 eV soft X-rays, for which the 18-41 Å wave-

lengths are large compared with internuclear distances, e.g., 1.098 Å for $N_2$ and 1.128 Å for CO [14]. The X-ray energies used in the present experiments, 13.5-14.5 keV, involve photon wavelengths of 0.86-0.92 Å that are smaller than internuclear distances, e.g., 2.281 Å for $Br_2$ [14]. The phase variations of the radiation field over the molecular geometry are therefore quite different between the soft X-ray and hard X-ray regimes. The theoretical calculation developed for the $N_2$ experiment [9,15] identified bond-length-dependent dipole and nondipole amplitudes as important factors. Similar considerations of molecular geometry were identified in understanding the wavelength dependence of nondipole interactions in resonant inelastic X-ray scattering experiments on molecules [16].

In summary, the nondipole asymmetries of Kr 1s and Br K-shell photoelectrons of $Br_2$ and $BrCF_3$ show similar variations with kinetic energy. The measured asymmetries agree well with independent-particle-approximation calculations of first-order retardation corrections for Kr 1s and Br 1s. The molecular Br K-shell asymmetries do not deviate significantly from the atomic model, in contrast with the "extra-atomic" effects measured for K-shells of $N_2$ and CO [9,10]. The ratio of photon wavelength to internuclear distance is suggested as a factor in explaining these results.

This work was supported by the Chemical Sciences, Geosciences, and Biosciences Division and the Advanced Photon Source by the Office of Basic Energy Sciences, Office of Science, U.S. Department of Energy, under Contract No. W-31-109-Eng-38. L.A.L. and R.H.P. are supported by National Science Foundation Grant No. 0201595.

## References

[1] Schmidt, V., 1992. Photoionization of atoms using synchrotron radiation. Rep. Prog. Phys. 55, 1483–1659.

[2] Becker, U., Shirley, D.A., 1996. VUV and Soft X-Ray Photoionization. Plenum, New York.

[3] Starace, A.F., 1982. Theory of atomic photoionization. In: Mehlhorn, W. (Ed.) Handbuch der Physik, Vol. 31. Springer-Verlag, Berlin, pp. 1–121.

[4] Amusia, M. Ya., 1990. Atomic Photoeffect. Plenum, New York.

[5] Cooper, J.W., 1993. Photoelectron-angular-distribution parameters for rare-gas subshells. Phys. Rev. A 47, 1841–1851.

[6] Dunford, R.W., Kanter, E.P., Krässig, B., Southworth, S.H., Young, L., 2004. Higher-order processes in X-ray photoionization and decay. Radiat. Phys. Chem. 70, 149–172.

[7] Hemmers, O., Guillemin, R., Lindle, D.W., 2004. Nondipole effects in soft X-ray photoemission. Radiat. Phys. Chem. 70, 123–147.

[8] Krässig, B., Bilheux, J.-C., Dunford, R.W., Gemmell, D.S., Hasegawa, S., Kanter, E.P., Southworth, S.H., Young, L., LaJohn, L.A., Pratt, R.H., 2003. Nondipole asymmetries of Kr 1s photoelectrons. Phys. Rev. A 67, 022707.

[9] Hemmers, O., Wang, H., Focke, P., Sellin, I.A., Lindle, D.W., Arce, J.C., Sheehy, J.A., Langhoff, P.W., 2001. Large nondipole effects in the angular distributions of K-shell photoelectrons from molecular nitrogen. Phys. Rev. Lett. 87, 273003.

[10] Hemmers, O.A., Wang, H., Lindle, D.W., Focke, P., Sellin, I.A., Mills, J.D., Sheehy, J.A., Langhoff, P.W., 2000. Beyond the dipole approximation: angular distribution effects in the 1s photoemission from small molecules. In: Dunford, R.W., Gemmell, D.S., Kanter, E.P., Krässig, B., Southworth, S.H., Young, L. (Eds.) X-Ray and Inner-Shell Processes. American Institute of Physics, Melville, NY, pp. 222–228.

[11] Bechler, A., Pratt, R.H., 1989. Higher retardation and multipole corrections to the dipole angular distribution of 1s photoelectrons at low energies. Phys. Rev. A 39, 1774–1779.

[12] Tseng, H.K., Pratt, R.H., Yu, S., Ron, A., 1978. Photoelectron angular distributions. Phys. Rev. A 17, 1061–1079.

[13] Dehmer, J.L., Dill, D., 1976. Molecular effects on inner-shell photoabsorption. K-shell spectrum of $N_2$. J. Chem. Phys. 65, 5327–5334.

[14] Huber, K.P., Herzberg, G., 1979. Molecular Spectra and Molecular Structure IV. Constants of Diatomic Molecules. Van Nostrand Reinhold, New York.

[15] Langhoff, P.W., Arce, J.C., Sheehy, J.A., Hemmers, O., Wang, H., Focke, P., Sellin, I.A., Lindle, D.W., 2001. On the angular distributions of electrons photoejected from fixed-in-space and randomly oriented molecules. J. Electron Spectrosc. Relat. Phenom. 114-116, 23–32.

[16] Mills, J.D., Sheehy, J.A., Ferrett, T.A., Southworth, S.H., Mayer, R., Lindle, D.W., Langhoff, P.W., 1997. Nondipole resonant X-ray Raman spectroscopy: polarized inelastic scattering at the K edge of $Cl_2$. Phys. Rev. Lett. 79, 383–386.